Cellulose (2021) 28:10013–10023
https://doi.org/10.1007/s10570-021-04149-2

ORIGINAL RESEARCH

Construction of cellulose/carboxymethyl chitosan hydrogels for potential wound dressing application

Yi Guo · Chuanyin Zhao · Chao Yan · Li Cui

Received: 19 April 2021 / Accepted: 13 August 2021 / Published online: 31 August 2021

Abstract In this study, novel cellulose/carboxymethyl chitosan (CMCS) composite hydrogels were prepared by blending cellulose and CMCS in LiOH/urea aqueous solutions, and then cross-linking with epichlorohydrin. The structure and morphology of the composite hydrogels were characterized by Fourier transform infrared spectroscopy, wide-angle x-ray diffraction, thermo-gravimetric analysis, and scanning electron microscopy. The results revealed that chemical cross-linking reaction between cellulose and CMCS occurred in the hydrogel. Moreover, CMCS contributed to the enhancement of pore size, whereas cellulose acted as a strong backbone in the hydrogel to support the pore wall. The compressive strength of the composite hydrogels was significantly improved from 39.2 ± 2.2 to 145.2 ± 2.8 kPa as a result of the increase in cellulose content, while the equilibrium swelling ratio increased rapidly from 33.8 to 154.2 g/g with the increase in CMCS content. The composite hydrogels showed no cytotoxicity towards L929 cells, suggesting good biocompatibility. All these results indicate that the proposed cellulose/CMCS composite hydrogels can be effectively used as wound dressing materials.

Keywords Natural polymer · Composite hydrogels · Antibacterial activity · Biocompatibility

Y. Guo · C. Zhao · C. Yan (✉) · L. Cui (✉)
Hubei Key Laboratory of Biomass Fibers and Eco-Dyeing and Finishing, Wuhan Textile University, Wuhan 430073, China
e-mail: yanchao@wtu.edu.cn

L. Cui
e-mail: cuili@wtu.edu.cn

Y. Guo
State Key Laboratory of Bio-Fibers and Eco-Textiles, Qingdao University, Qingdao 266071, China

Introduction

Recently, great efforts are being invested to develop new materials for healing damaged skin rapidly and relieving suffering (Rowan et al. 2015). Wound dressings have been developed from a simple plain textile strip to engineered composite materials such as gauzes, membranes, sponges, gels, hydrocolloids and hydrogels (Pinho and Soares 2018). As an ideal dressing material, it should be easy to apply and painlessly removed, absorb fluids and exudates effectively, exhibit haemostaticity, maintain a moist wound environment, show high gas permeation and prevent microbial infection (Cheng et al. 2019; Chen et al. 2018a, b; Capanema et al. 2018). Non-toxicity, favorable biocompatibility, high elasticity and adequate mechanical strength are the other desired properties of an ideal wound dressing material (Naseri et al. 2015).

Properties such as biodegradability, biocompatibility, similarity to macromolecules recognized by the

human body, and promoting cell growth make some natural polymers suitable for wide use in biomedical applications (Gonzalez et al. 2014). In the last decade, various natural polymers, such as polysaccharides and derivatives (chitin, chitosan, alginates, heparin and cellulose), proteoglycans, and proteins (collagen, gelatin, fibrin, keratin), have been developed as wound dressings (Mogoşanu and Grumezescu 2014; Ganesan 2017; Ye et al. 2018; Jayakumar et al. 2011; Clark 2018; Ge et al. 2018; Li et al. 2016; Deepachitra et al. 2014; Singaravelu et al. 2015).

Chitosan, a positively charged polysaccharide obtained by partial N-deacetylation of chitin, possesses unique properties including antibacterial activity, wound healing, and hemostasis. Therefore, it is widely used in commercial dressings such as Celox and Hemcon (Chen et al. 2018a, b; Pourshahrestani et al. 2017). However, the poor solubility of chitosan in neutral water limits its applications in biomedicine, and the chemical modification of chitosan requires toxic organic substances. Carboxymethyl chitosan (CMCS), a chitosan derivative with high solubility under physiological conditions, inherits the basic merits from chitosan making it a potential candidate for wound dressings. Wang et al. reported that CMCS coated carboxymethylated cotton showed better hemostatic capacity than cotton fabric (Wang et al. 2020). However, since the water-soluble polymers are too weak to be used directly for wound dressing or scaffolding application, many attempts have been made to increase the structural strength of CMCS. For example, CMCS films were crosslinked by microwave technique to enhance their dimensional integrity for possible use in wound care applications (Zhang et al. 2019). CMCS-based hydrogel reinforced with modified cellulose nanocrystal for deep burn wound healing was developed by Huang et al. (2018). The hydrogels exhibit high self-healing efficiency, injectability, good mechanical strength, and a high equilibrium swelling ratio of 350% while maintaining structural integrity. Furthermore, natural polymers such as gelatin have been combined with CMCS by radiation crosslinking, which could efficiently stabilize the hydrogel structure and prolong the degradation time. The resulting CMCS/gelatin hydrogel could induce granulation tissue formation and accelerate wound healing (Huang et al. 2013).

Due to their biocompatible and biodegradable properties, cellulose and its derivatives have also been developed as wound dressing materials (Harkins et al. 2014; Cheng et al. 2018; Capanema et al. 2018; Fawal et al. 2018). Moreover, cellulose with stiff molecular chain could be used effectively to strengthen the materials (Harkins et al. 2014; He et al. 2018). Thus, in the present work, cellulose was introduced as a backbone into CMCS matrix, and novel cellulose/CMCS composite hydrogels were fabricated for application as wound dressing material. Cellulose and CMCS were dissolved in LiOH/urea aqueous solution to construct macroporous hydrogels by using epichlorohydrin as cross-linker. The structure and morphology of cellulose/CMCS composite hydrogels were characterized by Fourier transform infrared (FT-IR) spectroscopy, wide-angle x-ray diffraction (WXRD), thermogravimetric analysis (TGA) and scanning electron microscopy (SEM). The swelling behavior and mechanical properties of the composite hydrogels were investigated and discussed. In addition, the hydrogels were evaluated for use as wound dressing material.

Experimental section

Materials

Cotton linter pulp was supplied by Hubei Chemical Fiber Co. Ltd. (Xiangfan, China). Its weight-average molecular weight (M_W) was determined to be 6.3×10^4 g/mol by static laser light scattering (DAWN DSP, Wyatt Technology Co., US) in NaOH/urea aqueous solution. Chitosan (CS, 5×10^4 g/mol, degree of deacetylation is 93%) was purchased from Qingdao Yunzhou Biochemistry Co., Ltd. (Qingdao, China). NaOH, isopropanol, ethanol, monochloroacetic acid, LiOH•H_2O, urea, epichlorohydrin (ECH) and all other reagents (Shanghai Chemical Reagent Co. Ltd., China) were analytical grade and used as received without further purification.

Preparation of CMCS

CMCS was prepared according to the method proposed by Wahid et al. (2017) with slight changes. Initially, to make CS swollen and alkalized, 1 g of unpurified chitosan was dispersed in isopropanol (20 mL) and 2 mL of 40 wt% NaOH aqueous solution

was added at room temperature. After alkalization for 2 h, 1.5 g monochloroacetic acid dissolved in 2 mL isopropanol was added dropwise for 30 min under continuous stirring and the reaction mixture was stirred for 2 h at 60 °C. The reaction was stopped by adding an excess of 70% ethanol, and then the reaction mixture was neutralized with 10% acetic acid. The product was filtered and washed several times with 70–90% ethanol. Finally, the obtained light yellow powder was dried and stored for further use. The degree of substitution of CMCS was about 0.70, which was determined by using the potentiometric titration method (Huang et al. 2015).

Preparation of the cellulose/CMCS composite hydrogels

The cellulose solution was prepared according to the previous report of He et al. (2018) as follows. First, 5 g cotton linter pulp was completely dissolved in 95 g precooled aqueous solution of 8 wt% LiOH•H_2O/15 wt% urea at −12.8 °C to obtain 5 wt% cellulose solution. CMCS was dissolved in the same solvent at room temperature to obtain 5 wt% CMCS solution. The cellulose and CMCS solutions were mixed, and 1 mL ECH as the crosslinking agent was added dropwise into 10 g solution in an ice bath under mechanical stirring for 30 min to obtain a homogeneous solution. The mixed solutions were kept at 5 °C for 12 h to form gels. Finally, the gels were washed with distilled water to obtain the hydrogel samples, which were coded as Gel0, Gel1, Gel2, Gel3, Gel4 and Gel5 according to cellulose/CMCS weight ratios of 10/0, 9/1, 8/2, 7/3, 6/4 and 5/5, respectively.

Characterization

The samples were freeze-dried, ground into powder, and vacuum-dried for 48 h at 60 °C before measurement. FT-IR spectra were obtained by the KBr disk technique using a Fourier-transform infrared spectrometer (Perkin Elmer Spectrum One, Wellesley, MA) in the wavelength range from 4000 to 400 cm^{-1}. The wide-angle X-ray diffraction (WAXD) patterns with Cu K_α radiation (λ = 0.15405 nm) at 40 kV and 30 mA were recorded on an XRD instrument (D8, Bruker AXS GmbH, Karlsruhe, Germany) in the 2θ range from 6° to 40° with scanning rate of 2°/min. Thermogravimetric analysis (TGA) was carried out on a NETZSCH STA 449C thermal analyzer (NETZSCH, Germany) at heating rate of 10 °C/min from room temperature to 500 °C under nitrogen atmospheres. Scanning electron microscope (SEM) images were collected using a JSM-6510 SEM (JEOL, Japan) at an accelerating voltage of 15 kV. The hydrogels swollen to equilibrium in distilled water at 37 °C for 24 h were frozen in liquid nitrogen, snapped immediately, and then freeze-dried using a lyophilizer. The cross-section of the hydrogels was sputtered with gold, observed, and photographed.

The compression strength of hydrogels in the equilibrium swelling state was measured on a universal tensile machine (CMT 6503, Shenzhen SANS, China) according to ISO527-3–1995 (E). The dimension of cylinder samples was about 10 mm (D) × 10 mm (H), and the crosshead speed was 2 mm/min. The results are averages of five measurements.

The gravimetric method was employed to measure the swelling ratios of the hydrogels in distilled water at 37 °C. The equilibrium swelling ratio (ESR) was calculated as

$$ESR = W_s/W_d \quad (1)$$

where W_s and W_d represent the weight of swollen hydrogel at swelling equilibrium and freeze-dried gel, respectively. All experiments were performed at least three times.

Water uptake (WU) was measured to evaluate the reswelling. To measure WU, the freeze-dried gels were immersed in distilled water at 37 °C. At regular time intervals, the samples were taken out and weighed after wiping excess water on the surface. The WU value was calculated as

$$\text{WU}\ (\%) = (W_t - W_d)/W_s' 100\% \quad (2)$$

where W_t is the weight of the re-swollen gel at time t, W_d and W_s are the same as in Eq. (1).

Antibacterial activity test

The antibacterial performance of the hydrogels was tested according to the previous report (Gonzalez et al. (2014)) to evaluate the resistance of the hydrogel against bacteria. Briefly, the dried Gel0, Gel2, Gel3 and Gel5 samples with diameter of 1 cm and height of 1 cm were sterilized for 30 min by UV on a clean

bench. The sterilized samples were placed on a solidified agar (Mueller–Hinton Agar, MHA). Then, 15 μL of a suspension of bacteria (*Staphylococcus aureus* CMCC 26,003 and *Echerichia coli* CMCC 44,102) with a concentration of 3.0×10^8 UFC/mL was dropped on the upper surface of hydrogels to culture at 37 °C for 24 h in an incubator. The cultured hydrogels were frozen in liquid nitrogen and snapped immediately, and then freeze-dried. The cross-section of the hydrogels was sputtered with gold, and then observed and photographed.

L929 cell viability assay

The cytotoxicity of hydrogels was evaluated through MTT assay. The freeze-dried hydrogels were ground into powder, sterilized by autoclaving, and then suspended in PBS at 1 mg/mL to culture, with 5000 cells in each well containing 200 μL Dulbecco's modified eagle medium (DMEM). After incubating for 48 h, 10 μL 3-[4,5-dimethylthiazole-2-yl]-2,5-diphenyltetrazolium bromide (MTT) was added in each well for a further 4 h incubation. Then, 200 μL DMSO was added to dissolve the formazan and the absorption intensity at 570 nm was detected. Cell viability was calculated using the following equation:

$$\text{Cell viability } (\%) = (A_{\text{test}}/A_{\text{control}}) \times 100\% \qquad (3)$$

where A_{test} and A_{control} correspond to the absorbance values of the test and control groups, respectively. In live/dead staining assay, 1 mg/mL hydrogel powder was added into the plate wells to culture at 48 h. After completion, 15 μL (2.5 μM) calcein acetoxymethyl ester (calcein-AM) and 9 μL (2.5 μM) propidium iodide (PI) were added into the wells to incubate for another 15 min at 37 °C/ 5% CO_2 atmosphere, and observed under fluorescent inverted microscope.

Results and discussion

Appearance and structure of the cellulose/CMCS composite hydrogels

Proposed mechanism for the cross-linking reaction of cellulose and CMCS with ECH in alkali aqueous solution is shown in Scheme 1. Figure 1 shows the photographs of the hydrogels at different states: the original hydrogels (Fig. 1a), the swollen hydrogels in distilled water (Fig. 1b), the dried hydrogels after vacuum-drying of the swollen hydrogels (Fig. 1c) and the dried hydrogels after swelling in physiological saline water for a week (Fig. 1d). Clearly, all original hydrogels (Fig. 1a) were homogeneous, transparent and relatively small, while the swollen hydrogels (Fig. 1b) grew in size with the increase in CMCS content. After vacuum-drying, the obtained dried hydrogels (Fig. 1c) with larger shrinkage became looser with the increase in CMCS content. The dried hydrogels were placed in physiological saline water for a week. Subsequently, the reswelling hydrogels (Fig. 1d) exhibited a certain mechanical strength which decreased with the increase in CMCS content from Gel0 to Gel5.

The FTIR spectra of the samples of chitosan, CMCS and the hydrogels are shown in Fig. 2. In the infrared spectrum of chitosan, a very strong and broad absorption peak was observed around 3437 cm^{-1}, which corresponded to O–H stretching and overlapped N–H stretching in the same region. The peaks at 2960–2870 cm^{-1} were due to symmetric and asymmetric C-H vibrations. The peaks at 1645 and 1599 cm^{-1} corresponded to amide I and II groups, respectively (Andrea et al. 2016). Compared with the FTIR spectrum of chitosan, CMCS showed the characteristic peaks at 1606 cm^{-1} and 1415 cm^{-1}, which corresponded to the respective asymmetric and symmetric stretching vibrations of $–COO^-$ (Wahid et al. 2017; Andrea et al. 2016). Furthermore, the C–O stretching band at 1030 cm^{-1} corresponding to the primary hydroxyl group of chitosan disappeared, which verified significant carboxymethylation of 6-OH (Zhou et al. 2015). The characteristic peak of second hydroxyl group at 1080 cm^{-1} was not changed. These results confirm the carboxymethylation of chitosan. Compared to the cellulose hydrogel without CMCS (Gel0, see Fig. 2b), intense peaks at 1627 cm^{-1} (N–H stretch) and 1418 cm^{-1} (C–O stretch) in the composite hydrogel indicated the presence of -NH_2 groups and –COOH groups, respectively (Kim et al. 2016). These results revealed that cellulose and CMCS were successfully crosslinked in the hydrogel.

The x-ray diffraction patterns of cellulose, CMCS and Gel3 were studied. As shown in Fig. 3, cellulose displayed distinct diffraction peaks at $2\theta = 14.8°$, 16.3° and 22.6°, which indicates the cellulose I

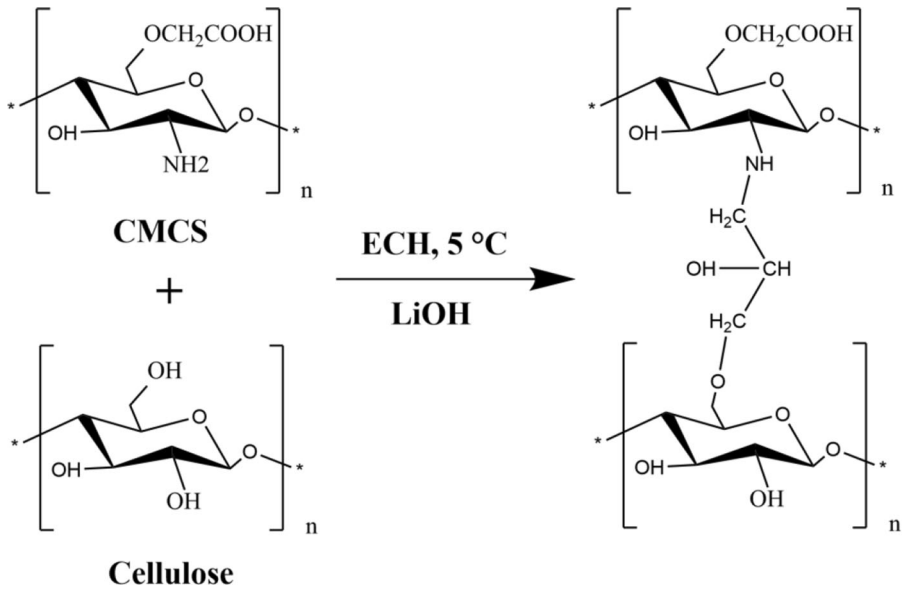

Scheme 1 Proposed mechanism for cross-linking reaction of cellulose and CMCS with ECH in LiOH/urea aqueous solution

crystalline form (French 2014). The diffraction pattern of pure CMCS showed a broad diffraction peak at $2\theta = 21.4°$, representing its amorphous structure (Yan et al. 2011). The WXRD characteristic peaks of cellulose and CMCS disappeared in the cellulose/CMCS hydrogels (Fig. 3c). It indicated that chemical cross-linking between cellulose and CMCS occurred in the hydrogel, leading to the destruction of the initial crystalline structure of cellulose and CMCS.

Thermogravimetric analysis (TGA) is a powerful technique to determine the polymers' state and evaluate the inter-molecular interaction between the two polymers in the composite materials. Figure 4 shows the TG and DTG curves for cellulose, CMCS, cellulose/CMCS mixture (weight ratio = 7:3) and Gel3 under N_2 atmosphere. The weight loss below 100 °C was due to the release of moisture from the samples. The peak around 270 °C of CMCS was attributed to the thermal decomposition of CMCS, whereas the peak at 350 °C of cellulose was caused by the decomposition of cellulose. The mixture of cellulose and CMCS exhibited two weight loss steps, which were assigned to the decomposition of CMCS and cellulose, respectively. However, there was only one weight loss step in the range of 220–380 °C for Gel3. This further indicated that chemical cross-linking between two polymers occurred in the hydrogel.

Figure 5 shows the SEM images of cross-sections of the freeze-dried swollen hydrogels. The cross-sections of the hydrogels displayed three-dimensional porous network structure. The average pore size of cellulose hydrogel regenerated from LiOH/urea aqueous solution (Gel0, see Fig. 5a) was about 20 to 30 μm. With increase in CMCS content, the average pore size of the composite hydrogels increased and exceeded 100 μm, leading to a more open and loose structure. These results indicated that the hydrophilic CMCS with –COOH groups contributed to the enhancement of pore size, whereas the relatively stiff cellulose acted as a backbone in the hydrogel to support the pore wall (Chang et al. 2010). Therefore, the composite hydrogels possessed higher swelling ratio.

Mechanical properties of the cellulose/CMCS composite hydrogels

The mechanical properties of cellulose and cellulose/CMCS composite hydrogels were also investigated. The results for the typical compressive modulus-strain curves of the hydrogels at room temperature are shown in Fig. 6. The compressive modulus of cellulose hydrogel was above 113.1 ± 8.1 kPa, which was much higher than that of previously reported cellulose hydrogels that were chemically cross-linked and

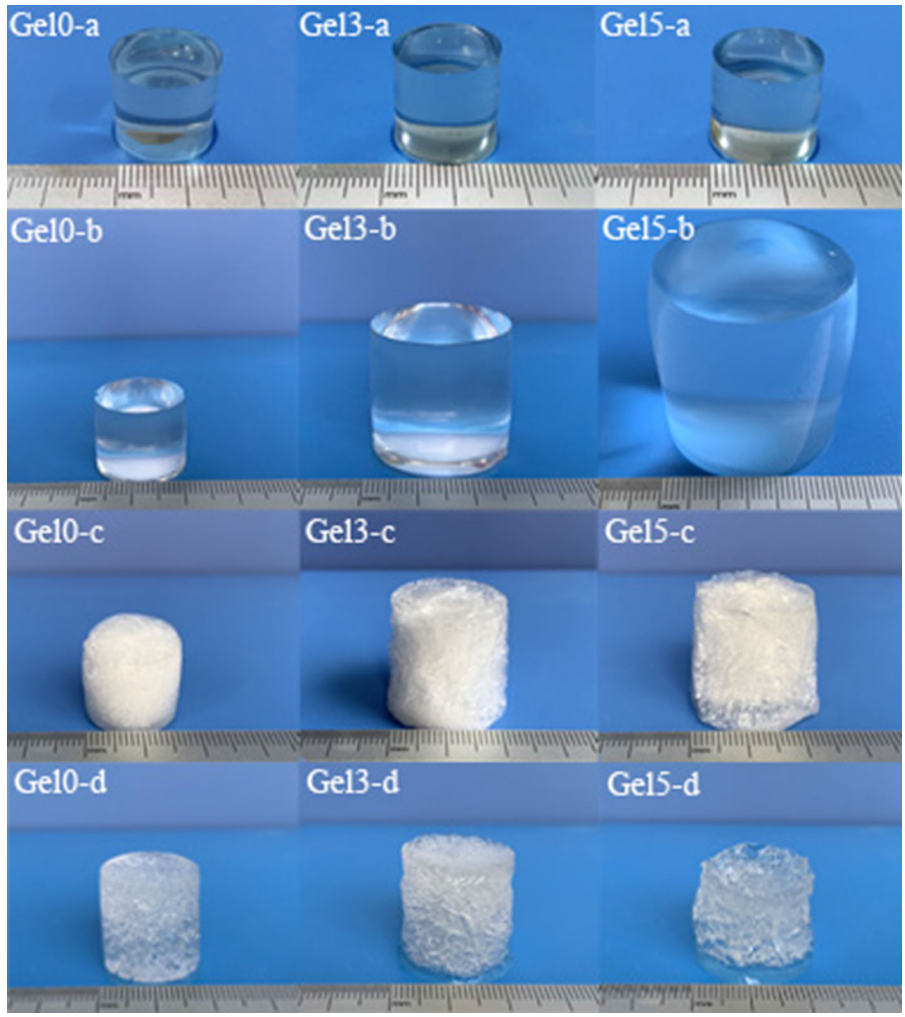

Fig. 1 Photographs of the hydrogels at different states: **a** original hydrogels, **b** swollen hydrogels, **c** dried hydrogels and **d** hydrogels after swelling in physical saline water for a week

regenerated from NaOH/urea aqueous solution (Chang et al. 2009). As expected, the mechanical strength of the composite hydrogels increased with an increase in cellulose content in the hydrogels. For example, the compressive modulus values of Gel5, Gel4, Gel3, Gel2 and Gel1 were 39.2 ± 2.2, 44.1 ± 3.9, 129.8 ± 1.2, 137.3 ± 2.7 and 145.2 ± 2.8 kPa, respectively. This further confirmed that cellulose played a key role in supporting the hydrogels, and could be used to improve the mechanical properties of CMCS. Therefore, according to the specific application, the mechanical properties of the composite hydrogels can be controlled by adjusting the cellulose content.

Figure 7 shows the influence of CMCS composition on the equilibrium swelling ratio of the composite hydrogels in distilled water at 37 °C. The composite hydrogels exhibited higher equilibrium swelling ratio than the cellulose hydrogel, indicating that the hydrophilic carboxyl group of CMCS could absorb a lot of water to enhance the water absorbing capacity of the hydrogels. With increase in the ratio of CMCS to cellulose in the hydrogels from 1:9 to 5:5, the equilibrium swelling ratio of the composite hydrogels increased rapidly from 33.8 to 154.2 g/g. This value is higher than that of previously reported self-healing hydrogel made of CMCS/dialdehyde-modified cellulose nanocrystal nanocomposite (Huang et al. 2018). The composite hydrogels with higher CMCS content

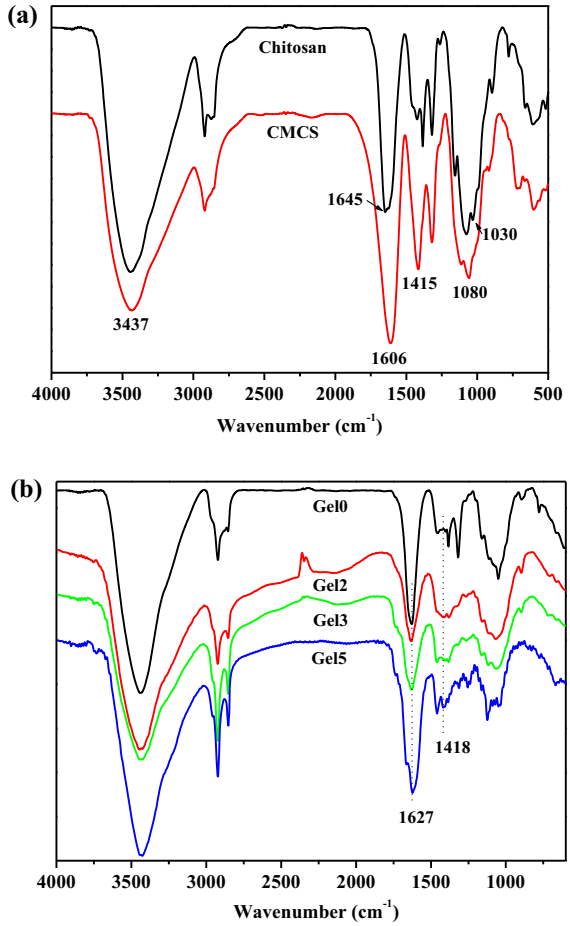

Fig. 2 FTIR spectra of **a** chitosan and CMCS, **b** the hydrogels

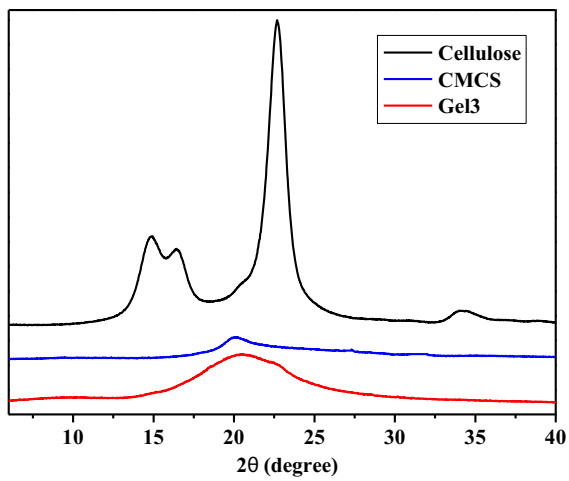

Fig. 3 X-ray diffraction patterns of cellulose, CMCS and Gel3

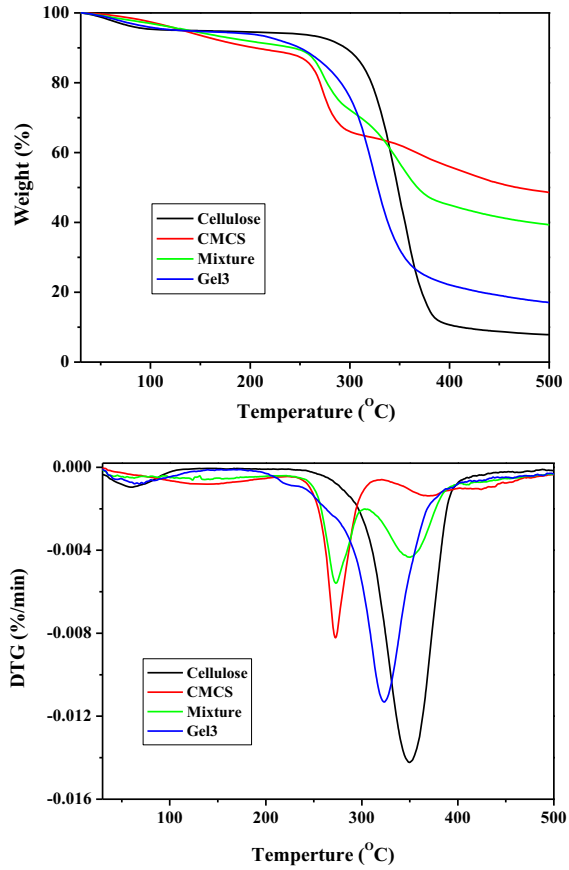

Fig. 4 TG and DTG curves of cellulose, CMCS, cellulose/CMCS mixture and Gel3

possessed higher ESR, resulting in the enhancement of the space in the hydrogels. This result further confirmed that CMCS acted as expander of pores, which was consistent with the results of SEM.

The reswelling behaviors of the freeze-dried hydrogels in distilled water at 37 °C are illustrated in Fig. 8. All hydrogels swelled in water very quickly during the first hour, then the swelling rates of the hydrogels became very slow, and all hydrogels finally reached the swelling equilibrium within about 4 h. The hydrogels presented a typical biphasic swelling pattern (Chang et al. 2009). The dried cellulose hydrogel showed only 18% water uptake. With increase in the ratio of CMCS to cellulose in hydrogels from 1:9 to 5:5, the water uptake of dried composite hydrogels increased from 24 to 58%. These results indicated that the reswelling capabilities of the composite hydrogels increased with increase in CMCS content, because the

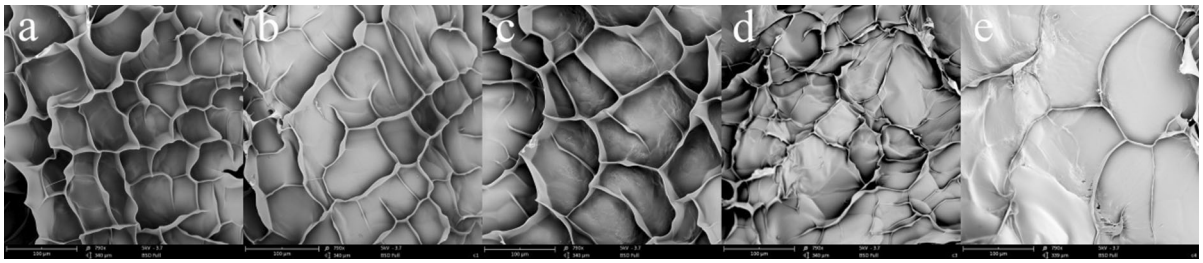

Fig. 5 SEM images of the cross-sections of the hydrogels: **a** Gel0, **b** Gel1, **c** Gel2, **d** Gel3 and **e** Gel4

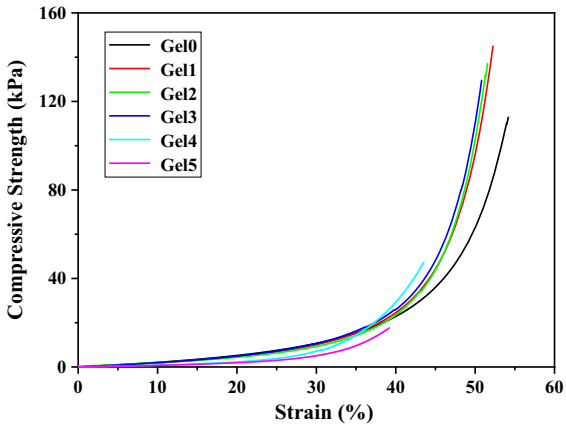

Fig. 6 Compressive modulus (σ)-strain (ε) curves of the hydrogels at room temperature

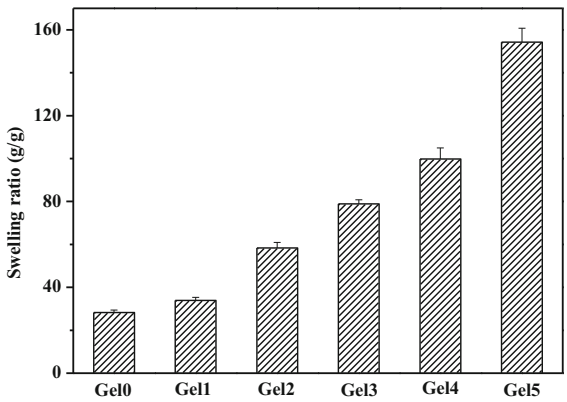

Fig. 7 Equilibrium swelling ratios of the hydrogels after immersing in distilled water for a week at 37 °C

larger pores could be preserved during the freeze-drying process.

The antibacterial activity of the composite hydrogels was evaluated by observing the growth of Gram positive and negative bacteria, *S. aureus* and *E. coli*, in the composite hydrogels. SEM images of the cross-

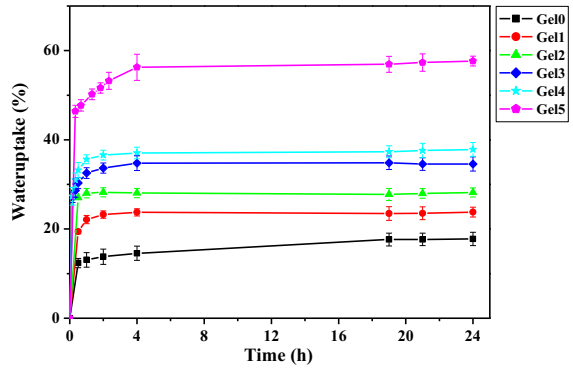

Fig. 8 Reswelling kinetic of the hydrogels in distilled water at 37 °C

sections of the composite hydrogels with different CMCS contents after culturing *S. aureus* for 24 h are shown in Fig. 9a–d, and larger magnification SEM images are presented in Fig. 9a'–c'. *S. aureus* bacteria colonies appeared on both the cellulose hydrogel (Fig. 9a, a') and the composite hydrogels (Fig. 9b, b', c, c'). Compared with the control sample, the number of bacteria colonies on the hydrogels decreased with the increase in CMCS content, and there were no bacteria colony on Gel5 (Fig. 9d). Thus, the antibacterial activity of the composite hydrogels against *S. aureus* apparently increased with the increase in CMCS content. The same results were obtained against *E. coli* c. Therefore, besides acting as expander of pore sizes, CMCS with -NH_2 groups can also play an antibacterial role in the composite hydrogels, which would prevent infection of wounds and accelerate wound healing.

MTT assay is widely used to investigate the cytotoxicity and biocompatibility of materials, which are important properties for wound dressing materials. Figure 10 shows the results of cytotoxicity of the composite hydrogels towards L929 cells. It was reported that crosslinked CMCS films prepared by

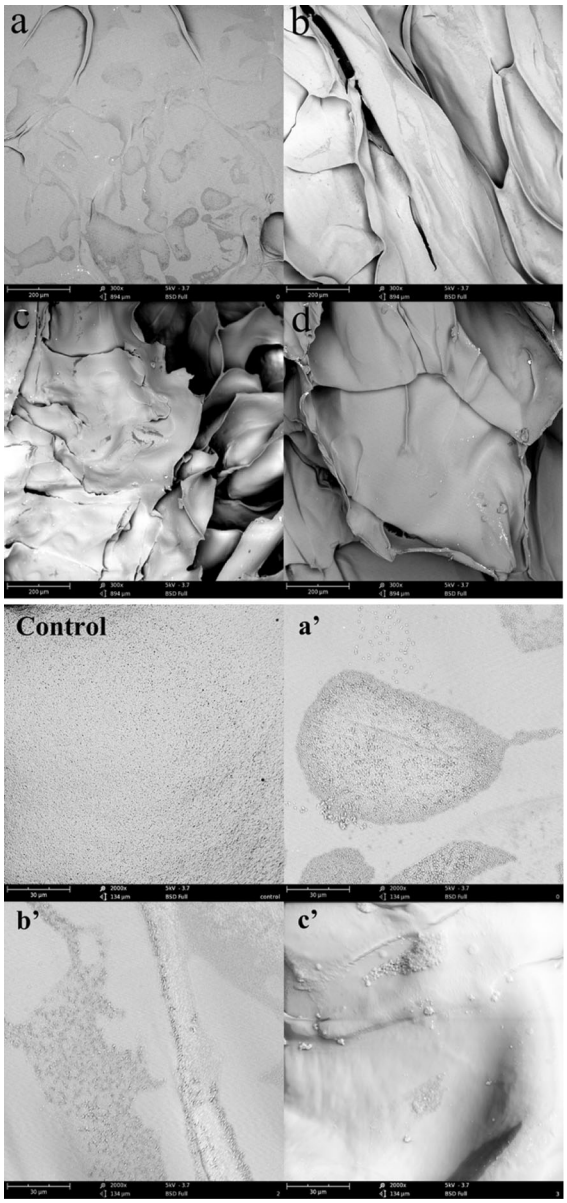

Fig. 9 SEM images of the cross-sections of the hydrogels after culturing *S. aureus* for 24 h: **a** Gel0, **b** Gel2, **c** Gel3, and **d** Gel5 (the scale bar is 200 μm); control, **a**' Gel0, **b**' Gel2 and **c**' Gel3 (the scale bar is 30 μm)

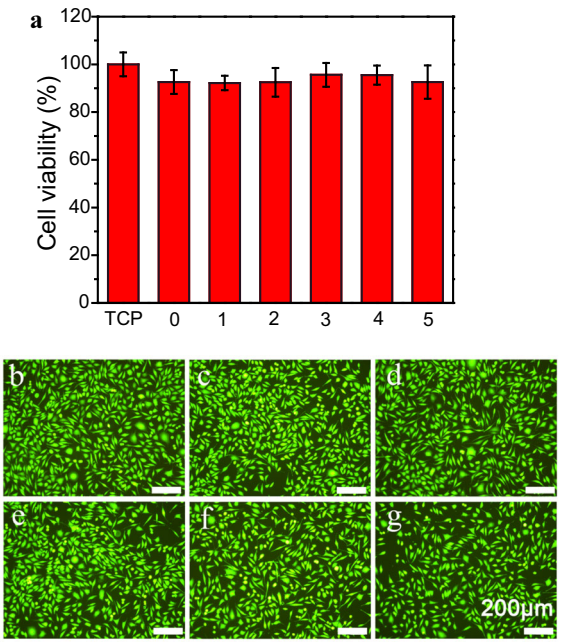

Fig. 10 The results of the cytotoxicity tests of hydrogels towards L929 cells after 48 h: **a** cell viability, and images of cells inside hydrogels observed by fluorescent inverted microscope: **b** control, **c** Gel1, **d** Gel2, **e** Gel3, **f** Gel4, and **g** Gel5. The scale bar is 200 μm

microwave treatment were cytotoxic (Wongpanit et al. 2005). In this study, the cell viabilities of the hydrogels with different CMCS contents presented no significant difference (Fig. 10a), which demonstrated the excellent cytocompatibility of the composite hydrogels. Moreover, normal cell morphology and uniform cell distribution were observed by fluorescent inverted microscope (see Fig. 10c–h), which further confirmed good biocompatibility of the composite hydrogels. Therefore, the proposed cellulose/CMCS composite hydrogels with excellent physicochemical properties, antibacterial activity and biocompatibility are suitable for prospective applications in wound healing.

Conclusions

Cellulose/CMCS composite hydrogels were successfully fabricated from LiOH/urea aqueous solution via cross-linking with epichlorohydrin. The composite hydrogels possessed macroporous structures and high equilibrium swelling ratio in water (above 154.2 g/g in water). The pore size, equilibrium swelling ratio and antibacterial activity of the composite hydrogels increased significantly with the CMCS content. The mechanical properties of the composite hydrogels were improved by cellulose, and the compressive modulus reached 145.2 ± 2.8 kPa. Moreover, the composite hydrogels exhibited no cytotoxicity towards L929 cells. The combination of cellulose

containing semi-stiff chain and CMCS containing –COOH and $–NH_2$ groups endowed the cellulose/CMCS composite materials with high equilibrium swelling ratio, excellent mechanical strength, good antibacterial activity and biocompatibility, suggesting their potential applications in wound dressing.

Acknowledgments This work was supported by open fund of State Key Laboratory of Bio-Fibers and Eco-Textiles (Qingdao University, No. KF2020205) as well as Scientific Research Programme of Hubei Provincial Department of Education (No. Q20171608). The authors gratefully thank Laboratory of Natural polymer and Polymer Physics (Wuhan University) for assistance with testing cytotoxicity.

Declarations

Conflict of interest The authors declare that they have no conflict of interest.

Research involving human participants and/or animals This article does not contain any studies with human participants or animals performed by any of the authors.

Informed Consent Informed consent was obtained from all individual participants included in the study.

References

Andrea L, Roberta S, Danilo M, Luciano M, Diego Palmiro R (2016) Optimization of carboxymethyl chitosan synthesis using response surface methodology and desirability function. Int J Biol Macromol 85:615–624. https://doi.org/10.1016/j.ijbiomac.2016.01.017

Capanema N, Mansur A, Jesus A, Carvalho S, Oliveira L, Mansur H (2018) Superabsorbent crosslinked carboxymethyl cellulose-PEG hydrogels for potential wound dressing applications. Int J Biol Macromol 106:1218–1234. https://doi.org/10.1016/j.ijbiomac.2017.08.124

Chang C, Duan B, Cai J, Zhang L (2010) Superabsorbent hydrogels based on cellulose for smart swelling and controllable delivery. Eur Polym J 46(1):92–100. https://doi.org/10.1016/j.eurpolymj.2009.04.033

Chang C, Duan B, Zhang L (2009) Fabrication and characterization of novel macroporous cellulose-alginate hydrogels. Polymer 50(23):5467–5473. https://doi.org/10.1016/j.polymer.2009.06.001

Chen J, Cheng W, Chen S, Xu W, Lin J, Liu H, Chen Q (2018a) Urushiol-functionalized mesoporous silica nanoparticles and their self-assembly into a Janus membrane as a highly efficient hemostatic material. Nanoscale 10(48):22818–22829. https://doi.org/10.1039/C8NR05882B

Chen Z, Han L, Liu C, Du Y, Hu X, Du G, Shan C, Yang K, Wang C, Li M, Li F, Tian F (2018b) A rapid hemostatic sponge based on large, mesoporous silica nanoparticles and N-alkylated chitosan. Nanoscale 10(43):20234–20245. https://doi.org/10.1039/c8nr07865c

Cheng F, Wu Y, Li H, Yan T, Wei X, Wu G, He J, Huang Y (2019) Biodegradable N, O-carboxymethyl chitosan/oxidized regenerated cellulose composite gauze as a barrier for preventing postoperative adhesion. Carbohyd Polym 207:180–190. https://doi.org/10.1016/j.carbpol.2018.10.077

Cheng H, Li C, Jiang Y, Wang B, Wang F, Mao Z, Xu H, Wang L, Sui X (2018) Facile preparation of polysaccharide-based sponges and their potential application in wound dressing. J Mater Chem B 6(4):634–640. https://doi.org/10.1039/C7TB03000B

Clark M (2018) Alginates in dressings and wound management. In: Rehm B, Moradali M (eds) Alginates and their biomedical applications. Springer Series in Biomaterials Science and Engineering, vol 11. Springer, Singapore, p 213 222. https://doi.org/10.1007/978-981-10-6910-9_8

Deepachitra R, Ramnath V, Sastry TP (2014) Graphene oxide incorporated collagen-fibrin biofilm as a wound dressing material. RSC Adv 4(107):62717–62727. https://doi.org/10.1039/C4RA10150B

Fawal G, Abu-Serie M, Hassan MA, Elnouby MS (2018) Hydroxyethyl cellulose hydrogel for wound dressing: Fabrication, characterization and in vitro evaluation. Int J Biol Macromol 111:649–659. https://doi.org/10.1016/j.ijbiomac.2018.01.040

French AD (2014) Idealized powder diffraction patterns for cellulose polymorphs. Cellulose 21:885–896. https://doi.org/10.1007/s10570-013-0030-4

Ganesan P (2017) Natural and bio polymer curative films for wound dressing medical applications. Wound Med 18:33–40. https://doi.org/10.1016/j.wndm.2017.07.002

Ge L, Xu Y, Li X, Yuan L, Tan H, Li D, Mu C (2018) Fabrication of antibacterial collagen-based composite wound dressing. ACS Sustain Chem Eng 6(7):9153–9166. https://doi.org/10.1021/acssuschemeng.8b01482

Gonzalez JS, Ludueña LN, Ponce A, Alvarez VA (2014) Poly(vinyl alcohol)/cellulose nanowhiskers nanocomposite hydrogels for potential wound dressings. Mat Sci Eng C-Mater 34:54–61. https://doi.org/10.1016/j.msec.2013.10.006

Harkins AL, Duri S, Kloth LC, Tran CD (2014) Chitosan-cellulose composite for wound dressing material. Part 2. Antimicrobial activity, blood absorption ability, and biocompatibility. J Biomed Mater Res Part B Appl Biomater 102(6):1199–1206. https://doi.org/10.1002/jbm.b.33103

He M, Chen H, Zhang X, Wang C, Xu C, Xue Y, Wang J, Zhou P, Zhao Q (2018) Construction of novel cellulose/chitosan composite hydrogels and films and their applications. Cellulose 25:1987–1996. https://doi.org/10.1007/s10570-018-1683-9

Huang W, Wang Y, Huang Z, Wang X, Chen L, Zhang Y, Zhang L (2018) On-demand dissolvable self-healing hydrogel based on carboxymethyl chitosan and cellulose nanocrystal for deep partial thickness burn wound healing. ACS Appl Mater Interfaces 10(48):41076–41088. https://doi.org/10.1021/acsami.8b14526

Huang X, Zhang Y, Zhang X, Xu L, Chen X, Wei S (2013) Influence of radiation crosslinked carboxymethyl-chitosan/gelatin hydrogel on cutaneous wound healing. Mat Sci Eng

C-Mater 33(8):4816–4824. https://doi.org/10.1016/j.msec.2013.07.044

Huang Y, Huang J, Cai J, Lin W, Lin Q, Wu F, Luo J (2015) Carboxymethyl chitosan/clay nanocomposites and their copper complexes: Fabrication and property. Carbohyd Polym 134:390–397. https://doi.org/10.1016/j.carbpol.2015.07.089

Jayakumar R, Prabaharan M, Sudheesh Kumar P, Nair S, Tamura H (2011) Biomaterials based on chitin and chitosan in wound dressing applications. Biotechnol Adv 29(3):322–337. https://doi.org/10.1016/j.biotechadv.2011.01.005

Kim HR, Jang JW, Park JW (2016) Carboxymethyl chitosan-modified magnetic-cored dendrimer as an amphoteric adsorbent. J Hazard Mater 317:608–616. https://doi.org/10.1016/j.jhazmat.2016.06.025

Li HY, Wang MC, Williams GR, Wu J, Sun X, Lv Y, Zhu L (2016) Electrospun gelatin nanofibers loaded with vitamins A and E as antibacterial wound dressing materials. RSC Adv 6(55):50267–50277. https://doi.org/10.1039/C6RA05092A

Mogoşanu GD, Grumezescu MA (2014) Natural and synthetic polymers for wounds and burns dressing. Int J Pharmaceut 463(2):127–136. https://doi.org/10.1016/j.ijpharm.2013.12.015

Naseri N, Mathew A, Girandon L, Fröhlich M, Oksman K (2015) Porous electrospun nanocomposite mats based on chitosan-cellulose nanocrystals for wound dressing: effect of surface characteristics of nanocrystals. Cellulose 22:521–534. https://doi.org/10.1007/s10570-014-0493-y

Wongpanit P, Sanchavanakit N, Pavasant P, Supaphol P, Tokura S, Rujiravanit R (2005) Macromol Biosci 5:1001–1012. https://doi.org/10.1002/mabi.200500081

Pinho E, Soares G (2018) Functionalization of cotton cellulose for improved wound healing. J Mater Chem B 6(13):1887–1889. https://doi.org/10.1039/C8TB00052B

Pourshahrestani S, Zeimaran E, Kadri NA, Gargiulo N, Jindal HM, Naveen SV, Sekaran SD, Kamarul T, Towler MR (2017) Potency and cytotoxicity of a novel gallium-containing mesoporous bioactive glass/chitosan composite scaffold as hemostatic agents. ACS Appl Mater Interfaces 9(37):31381–31392. https://doi.org/10.1021/acsami.7b07769

Rowan MP, Cancio LC, Elster EA, Burmeister DM, Rose LF, Natesan S, Chan RK, Christy RJ, Chung KK (2015) Burn wound healing and treatment: Review and advancements. Crit Care 19:243. https://doi.org/10.1186/s13054-015-0961-2

Singaravelu S, Ramanathan G, Raja MD, Barge S, Sivagnanam UT (2015) Preparation and characterization of keratin-based biosheet from bovine horn waste as wound dressing material. Mater Lett 152:90–93. https://doi.org/10.1016/j.matlet.2015.03.088

Wahid F, Wang H, Zhong C, Chu L (2017) Facile fabrication of moldable antibacterial carboxymethyl chitosan supramolecular hydrogels cross-linked by metal ions complexation. Carbohyd Polym 165:455–461. https://doi.org/10.1016/j.carbpol.2017.02.085

Wang Y, Xiao D, Zhong Y, Zhang L, Chen Z, Sui X, Wang B, Feng X, Xu H, Mao Z (2020) Facile fabrication of carboxymethyl chitosan/paraffin coated carboxymethylated cotton fabric with asymmetric wettability for hemostatic wound dressing. Cellulose 27:3443–3453. https://doi.org/10.1007/s10570-020-02969-2

Yan S, Yin J, Tang L, Chen X (2011) Novel physically cross-linked hydrogels of carboxymethyl chitosan and cellulose ethers: Structure and controlled drug release behavior. J Appl Polym Sci 119(4):2350–2358. https://doi.org/10.1002/app.32678

Ye S, Jiang L, Wu J, Su C, Huang C, Liu X, Shao W (2018) Flexible amoxicillin-grafted bacterial cellulose sponges for wound dressing: In vitro and in vivo evaluation. ACS Appl Mater Interfaces 10(6):5862–5870. https://doi.org/10.1021/acsami.7b16680

Zhang W, Xin Y, Yin B, Ye G, Wang J, Shen J, Li L, Yang Q (2019) Synthesis and properties of crosslinked carboxymethyl chitosan and its hemostatic and wound healing effects on liver injury of rats. J Biomater Appl. https://doi.org/10.1177/0885328219852888

Zhou H, Cao P, Li J, Zhang F, Ding P (2015) Preparation and release kinetics of carboxymethyl chitosan/cellulose acetate microspheres as drug delivery system. J Appl Polym Sci 132(26):42152. https://doi.org/10.1002/app.42152